Defective vascular morphogenesis and mid-gestation embryonic death in mice lacking RA-GEF-1

Ping, Wei ; Satoh, Takaya ; Edamatsu, Hironori ; Aiba, Atsu ; Setsu, Tomiyoshi ; Terashima, Toshio ; Kitazawa, Sohei ; Nakao, Kazuki ;…

(Citation)
Biochemical and Biophysical Research Communications,363(1):106-112

(Issue Date)
2007-11-09

(Resource Type)
journal article

(Version)
Accepted Manuscript

(URL)
https://hdl.handle.net/20.500.14094/90001682

Defective Vascular Morphogenesis and Mid-gestation Embryonic Death in Mice Lacking RA-GEF-1

Ping Wei[a], Takaya Satoh[a], Hironori Edamatsu[a], Atsu Aiba[b], Tomiyoshi Setsu[c], Toshio Terashima[c], Sohei Kitazawa[d], Kazuki Nakao[e], Yoko Yoshikawa[a], Masako Tamada[a], and Tohru Kataoka[a*]

[a]Division of Molecular Biology, Department of Biochemistry and Molecular Biology, [b]Division of Molecular Genetics, Department of Physiology and Cell Biology, [c]Division of Developmental Neurobiology, Department of Physiology and Cell Biology, [d]Division of Molecular Pathology, Department of Pathology and Microbiology, Kobe University Graduate School of Medicine, 7-5-1 Kusunoki-cho, Chuo-ku, Kobe 650-0017, Japan, [e]Laboratory of Animal Resources and Genetic Engineering, Riken Center for Developmental Biology, Kobe 650-0047, Japan.

[*]Corresponding author. Fax: +81-78-382-5399, E-mail address: kataoka@people.kobe-u.ac.jp.

Keywords: angiogenesis, embryonic lethality, knockout mouse, RA-GEF-1, Rap1, vasculogenesis.

Abstract

A multitude of guanine nucleotide exchange factors (GEFs) regulate Rap1 small GTPases, however, their individual functions remain obscure. Here, we investigate the *in vivo* function of the Rap1 GEF RA-GEF-1. The expression of RA-GEF-1 in wild-type mice starts at embryonic day (E) 8.5, and continues thereafter. *RA-GEF-1*$^{-/-}$ mice appear normal until E7.5, but become grossly abnormal and dead by E9.5. This mid-gestation death appears to be closely associated with severe defects in yolk sac blood vessel formation. *RA-GEF-1*$^{-/-}$ yolk sacs form apparently normal blood islands by E8.5, but the blood islands fail to coalesce into a primary vascular plexus, indicating that vasculogenesis is impaired. Furthermore, *RA-GEF-1*$^{-/-}$ embryos proper show severe defects in the formation of major blood vessels. These results suggest that deficient Rap1 signaling may lead to defective vascular morphogenesis in the yolk sac and embryos proper.

Rap1 belongs to the Ras family of small GTPases, and is implicated in regulation of a variety of cellular phenomena such as proliferation, adhesion, and exocytosis [1]. In particular, many *in vitro* experiments have shown that Rap1 is involved in integrin-mediated adhesion [2]. Recent studies employing gene targeting of individual Rap1 members also support this notion [3,4].

In response to extracellular stimuli, Rap1 activity is regulated through the action of specific guanine nucleotide exchange factors (GEFs) including C3G, Epacs, CalDAG-GEFs, RA-GEFs (PDZ-GEFs), and phospholipase Cε [1]. Two related GEFs called RA-GEF-1 (also called PDZ-GEF1, nRapGEP and CNRasGEF) [1,5,6] and RA-GEF-2 [7] are characterized by possession of both PSD-95/DlgA/ZO-1 (PDZ) and Ras/Rap-associating (RA) domains. Through the interaction with Rap1-GTP, RA-GEF-1 co-localizes with Rap1 at the Golgi complex, leading to the amplification of the Rap1-mediated signaling [6]. On the other hand, RA-GEF-2 is recruited to the plasma membrane by association with M-Ras-GTP [7].

In vivo functions of Rap1 GEFs have been analyzed by gene targeting. Mice lacking C3G show embryonic lethality shortly after implantation [8]. In contrast, mice lacking CalDAG-GEFI are viable, but their platelets are severely compromised in integrin-dependent aggregation [9]. Recently, we have generated RA-GEF-2 knockout mice, in which tumor necrosis factor-α-dependent integrin activation and adhesion were impaired specifically in splenic B cells [10]. However, no mouse model that exhibits embryonic vascular abnormalities due to deficient Rap1 signaling has been reported.

In this study, we have generated mice with functional disruption of the *RA-GEF-1* allele and found that *RA-GEF-1*$^{-/-}$ mice show mid-gestation embryonic lethality, which is closely associated with severe defects in embryonic vasculogenesis.

Materials and methods

Construction of the targeting vector. An *RA-GEF-1* genomic DNA fragment was cloned from a 129/Sv mouse genomic bacterial artificial chromosome library (Invitrogen, Carlsbad, CA). Exon 15 of the *RA-GEF-1* gene was flanked with a loxP site at its 5' end and loxP-neomycin-resistant cassette (*TK-neo*)-loxP at its 3' end (Fig. 1A). The resulting vector contains the 5' and 3' arms of 7.1-kb and 4.1-kb RA-GEF-1 genomic sequences, respectively, for homologous recombination.

Gene targeting and generation of mutant mice. Mouse EB3 embryonic stem (ES) cells were electroporated with the *Not*I-linearized targeting construct. ES cell clones carrying the properly generated *RA-GEF-1*^{flox} allele were microinjected into C57BL/6 blastocysts. Male chimeras were bred with C57BL/6 females to generate *RA-GEF-1*$^{flox/+}$ mice. *RA-GEF-1*$^{+/-}$ mice were generated by crossing *RA-GEF-1*$^{flox/+}$ mice to *CAG-cre* transgenic mice [11]. Embryos were harvested from timed mating between *RA-GEF-1*$^{+/-}$ mice.

Genotyping. The genotypes of the mutant mice were determined within 3 weeks after birth by Southern blot and polymerase chain reaction (PCR) analyses of their tail DNAs as described previously [12]. For genotyping by PCR, the following three primers were used; p1 (5'-GTCAGACTAGCAGCAGACCACCTAG-3'), p2

(5'-GCGTGTGTTGGAGGTTATCCCAG-3'), and p3 (5'-CGAGTCCTGAACATAAGGGCAGGG-3') (Fig. 1A). PCR genotyping of embryos later than E8.5 was done by using DNA isolated from their extraembryonic membranes.

Western blot analysis. Western blot analysis was performed as described [12,13] with affinity-purified rabbit anti-RA-GEF-1 antibody raised against a synthetic peptide of the C-terminal 21 residues of mouse RA-GEF-1 (CDADPRLAPFQPQGFAGAE ED) (Operon Biotechnologies, Tokyo, Japan). Anti-mouse α-actin antibody (Santa Cruz Biotechnology, Santa Cruz, CA) was used as a loading control.

Reverse transcription (RT)-PCR. The total cellular RNA was prepared from whole embryos, and RT-PCR was done as described previously [13]. The following primers were used for amplification of the RA-GEF-1 mRNA: 5'-CCACGGTGCCACTGAGAGCCAGTGC-3' and 5'-AGGTGCCGGTGAAGGATCTGCCTCC-3'.

Histological analysis. Embryos were embedded in paraffin, sectioned (4-μm), and stained with hematoxylin and eosin (HE). Whole-mount immunostaining of embryos and yolk sacs was performed as described previously [14] using anti-mouse platelet endothelial cell adhesion molecule-1 (PECAM-1) antibody (BD Biosciences-pharmigen. San Diego, CA) and horseradish peroxidase-conjugated sheep anti-rat immunoglobulin G (IgG) antibody (GE Healthcare Bio-Sciences, Piscataway, NJ). For immunofluorescence staining, yolk sacs were embedded in OCT compound (Tissue-Tek, Miles, Elkhart, IN), sectioned, and stained with primary antibody against RA-GEF-1 or PECAM-1, followed by Alexa Fluor 488-labeled anti-rabbit IgG (Molecular Probes, A-11034) or Alexa Fluor 546-labeled anti-rat IgG (Molecular Probes, A-11081) antibodies. Fluorescence was detected by confocal laser scanning microscopy (LSM510 META; Carl Zeiss, Jena, Germany).

Results

Generation of the RA-GEF-1 null allele

The *RA-GEF-1*^{flox} allele was created in mouse 129/Ola-derived ES cells by homologous

recombination (Fig. 1A). One out of 95 G418-resistant ES cell clones was verified to carry the *RA-GEF-1*^{flox} allele (Fig. 1B). This ES clone was used to derive *RA-GEF-1*$^{flox/+}$ mice, whose genotypes were verified by Southern blot hybridization and PCR (Fig. 1C). Subsequently, the *RA-GEF-1*$^{-}$ allele was generated through Cre-mediated deletion of exon15-loxP-*TK-neo* (Fig. 1C). Embryo genotypes were determined by PCR using allele-specific primers as exemplified in Fig. 1D.

Embryonic lethality of RA-GEF-1$^{-/-}$ *mice*

No newborn *RA-GEF-1*$^{-/-}$ pups were present after examining 174 pups from the cross-breeding of *RA-GEF-1*$^{+/-}$ mice, indicating that RA-GEF-1 deficiency results in embryonic lethality (Table 1). *RA-GEF-1*$^{+/-}$ mice were born at a normal Mendelian ratio and appeared healthy and fertile (Table 1 and data not shown). *RA-GEF-1*$^{-/-}$ embryos appeared normal until E7.5 with normal development of the three embryonic germ layers and amnion (data not shown). At E8.5, *RA-GEF-1*$^{-/-}$ embryos were observed at the expected Mendelian ratio (Table 1). However, they exhibited variable appearances ranging from apparently normal (Fig. 2A, *middle panel*) to noticeably reduced in size with no embryonic turning (Fig. 2A, *right panel*). At E9.5, *RA-GEF-1*$^{-/-}$ embryos appeared grossly abnormal with reduced sizes and undulated neural tubes without closure of the anterior and posterior pores. They were arrested in development after forming 15 somites without completion of embryonic turning (Fig. 2B). Furthermore, E9.5 *RA-GEF-1*$^{-/-}$ embryos had pale yolk sacs lacking obvious blood vessels, whereas yolk sacs of all E9.5 wild-type embryos exhibited large vitelline blood vessels filled with blood, suggesting a gross abnormality in blood vessel formation in *RA-GEF-1*$^{-/-}$ embryos (Fig. 2C). At E10.5-12.5, they were deteriorated and completely absorbed at around E13.5 (Table 1).

Expression of RA-GEF-1 in mouse embryos

Western blot analysis confirmed the expression of RA-GEF-1 in E10.5 wild-type embryos as a major 160 kDa band, which was not observed in *RA-GEF-1*$^{-/-}$ embryos (Fig. 2D). The expression of RA-GEF-1 was undetectable until E7.5 but exhibited a marked

increase at E8.5, when abnormal vascular development seems to start in *RA-GEF-1*$^{-/-}$ mice (Fig. 2E). The spatial expression pattern of RA-GEF-1 in E8.5 yolk sacs was examined by immunofluorescence staining (Fig. 2F). RA-GEF-1 was widely expressed with strong expression at vascular endothelial cells positive for PECAM-1.

Defective vascular development in RA-GEF-1$^{-/-}$ *embryos*

We visualized the vascular network of E9.5 *RA-GEF-1*$^{-/-}$ and wild-type embryos by whole-mount immunostaining with anti-PECAM-1 antibody. At E9.5, wild-type embryos showed well-organized blood vessels such as dorsal aortae, aortic arches, cranial vessels and intersomitic vessels (Fig. 3A, *left panel*). In contrast, *RA-GEF-1*$^{-/-}$ embryos showed varying vascular morphology. Most of them lacked major blood vessels but possessed delicate plexus-like structures at the site of dorsal aortae, suggesting a severe defect in vasculogenesis (Fig. 3A, *middle panel*). Three out of 12 embryos examined had an abnormal balloon-shaped allantois strongly positive for PECAM-1 (Fig. 3A, *right panel*). The vasculature of these embryos was less severely affected, and structures like dorsal aortae and intersomitic vessels were visible albeit hypomorphic. The balloon-shaped allantois phenotype showed remarkable similarity to that of mice deficient in α_4 integrin [15] or VCAM-1 [16].

Defective vascular development in RA-GEF-1$^{-/-}$ *yolk sacs*

The yolk sac vasculature is initiated with the development of blood islands derived from distinct mesodermal cells around E8.0 [17]. The blood islands fuse with each other and form lumina, eventually leading to formation of a primitive vascular plexus by E8.75. Subsequently, large vitelline vessels and a meshwork of smaller vessels arise from the existing capillary plexus around E9.5 by angiogenic vascular remodeling. We visualized the vascular network in yolk sacs with PECAM-1 immunostaining. E9.5 wild-type yolk sacs showed formation of large vitelline collecting vessels and a network of smaller vessels (Fig. 3B). In striking contrast, in *RA-GEF-1*$^{-/-}$ yolk sacs, blood islands surrounded by PECAM-1-positive vascular endothelium were visible, but they failed to coalesce to form a honeycomb-like primitive vascular plexus, indicating a failure in vasculogenesis (Fig. 3B).

We next analyzed sections of yolk sacs by HE staining. At E8.5, blood islands formed in *RA-GEF-1*$^{-/-}$ yolk sacs were indistinguishable from those in wild-type, in which fetal nucleated erythrocytes were surrounded by an endothelial layer forming close contacts between visceral endodermal and mesodermal layers, indicating that hematopoiesis was not disturbed (Fig. 3C, *a-d*). By E9.5, the large vitelline collecting vessels and the small capillary branching vessels were well differentiated and filled with erythrocyte in the wild-type yolk sacs (Fig. 3C, *e* and *g*). In contrast, in *RA-GEF-1*$^{-/-}$ yolk sacs, the blood islands were occasionally dilated, and the endodermal layer exhibited a characteristic buckling appearance, which could be due to disruption of endothelial cell adhesion as observed in mice deficient in transforming growth factor-β1 [18] (Fig. 3C, *f* and *h*). Moreover, they contained smaller number of erythrocytes, which was consistent with the pale appearance of *RA-GEF-1*$^{-/-}$ yolk sacs (Fig. 2C). These results suggest that RA-GEF-1 plays a crucial role in the late stage of vasculogenesis (formation of a primitive vascular plexus), but not in the earlier step (formation of blood islands) in yolk sacs.

Defective vascular development in RA-GEF-1$^{-/-}$ *placentas*

Histological analysis of placentas from *RA-GEF-1*$^{-/-}$ conceptuses also showed abnormal vascular development. In normal development, after the attachment of allantois to chorion, the allantoic vessels undergo further angiogenesis to invade the chorionic plate by E8.5 and form a labyrinthine layer, where embryonic blood vessels are intertwined with maternal lacunae by E9.5 [19]. At E9.5, the labyrinthine layer of wild-type placentas possesses dense networks of embryonic vessels containing nucleated erythrocytes (Fig. 3D). In contrast, the labyrinthine layer of *RA-GEF-1*$^{-/-}$ placentas was markedly reduced in thickness and much less vascularized with embryonic vessels (Fig. 3D). Embryonic vessels of *RA-GEF-1*$^{-/-}$ placentas also contained smaller number of erythrocytes.

Discussion

During embryogenesis, the vascular system is formed by two main processes,

vasculogenesis and angiogenesis. In vasculogenesis, the endothelial cells differentiate from endothelial progenitor cells and coalesce into a primary vascular plexus. During angiogenesis, the primitive vasculature is remodeled to form the more complex vasculature [17, 20]. We demonstrate that blood island formation and hematopoiesis are not affected until E8.5, but blood islands fail to fuse with each other to form a primary vascular plexus by E9.5 in *RA-GEF-1*$^{-/-}$ yolk sacs, which is compatible with the temporal pattern of RA-GEF-1 expression that starts around E8.5. Given almost no *RA-GEF-1*$^{-/-}$ embryos survive beyond E9.5, the failure in yolk sac vasculature may be the primary cause of their mid-gestation death because the yolk sac serves nutritive and metabolic functions to ensure normal development of the embryo before the functional placenta is formed around E10.5.

One notable feature of the *RA-GEF-1*$^{-/-}$ embryos proper is considerable difference in the severity of the vascular phenotypes observed at E9.5. Only the local primitive vascular networks are observed in severely affected *RA-GEF-1*$^{-/-}$ embryos, however, the hypomorphic dorsal aortae and intersomitic vessels are visible in less affected ones (Fig. 3A). This high extent of variability could be due to asynchrony of development, which may arise from the mixed genetic background of the mice (129/Ola × C57BL/6). Alternatively, the defective vascular development in *RA-GEF-1*$^{-/-}$ embryos proper may be secondary to the embryonic death caused by the overall failure of the yolk sac vasculature. Likewise, the observed abnormalities in *RA-GEF-1*$^{-/-}$ embryos, such as growth retardation, defective neural tube closure and incomplete embryonic turning, may also reflect the failure of the yolk sac vasculature.

Interestingly, 3 out of 12 E9.5 *RA-GEF-1*$^{-/-}$ embryos had a large, swollen allantois which is not connected to the chorion. Similar abnormal development of the allantois is observed in mouse embryos lacking α4 integrin [15] or its counter receptor, VCAM-1 [16]. α4 integrin and VCAM-1 are normally expressed in a reciprocal pattern in the chorion and allantois, and the interaction of the two counter receptors is required for formation of the chorioallantois. Thus, RA-GEF-1 might regulate Rap1 that is involved in α4 integrin-VCAM-1-dependent chorioallantoic fusion. The vascular defects in *RA-GEF-1*$^{-/-}$ embryos are also manifested in the placentas. However, it is presently unclear whether the phenotypes are due to impaired

angiogenic sprouting or simply a consequence of defective blood vessel formation at these sites.

In this paper, we have demonstrated that RA-GEF-1 plays a crucial role in embryonic vascular development. To our knowledge, this is the first demonstration of deficient vasculogenesis in mice lacking Rap1 signaling molecules. However, mechanisms underlying RA-GEF-1-dependent vasculogenesis remain unclear. RA-GEF-1 associates with the adaptor protein MAGI-1, which is required for the cell-cell contact-dependent Rap1 activation and enhancement of VE-cadherin-mediated cell adhesion [21,22]. Thus, RA-GEF-1/MAGI-1 interaction may have a role in vasculogenesis in mice. It is also noteworthy that orthologs of RA-GEFs, such as PXF-1 in *Caenorhabditis elegans* and Dizzy in *Drosophila melanogaster*, play an important role to regulate cell-cell and cell-matrix adhesions [23,24]. Vasculogenesis defects in yolk sacs were also observed in mice lacking fibronectin, α5 integrin, VE-cadherin, or N-cadherin, suggesting that abnormal vasculogenesis observed in *RA-GEF-1*$^{-/-}$ mice may be ascribed to impaired cell adhesion mediated by integrins and cadherins downstream of Rap1 [25-28]. Further studies employing tissue- or cell-type-specific RA-GEF-1 knockout mice and cultured vascular endothelial cells will be necessary to elucidate the molecular mechanisms.

Acknowledgment

We are grateful to Dr. Hitoshi Niwa for providing ES cells, Dr. Jun-ichi Miyazaki for providing *CAG-cre* transgenic mice, Dr. Kenji Araishi for valuable experimental assistance, and Dr. Shuji Ueda for variable advice. This work was supported by Grants-in-Aid for Scientific Research in Priority Areas 17014061 and 18016018 and for Scientific Research 17390078, 17370050 and 18790223, and by a 21st Century COE Program from the Ministry of Education, Science, Sports and Culture of Japan.

References

[1] J. L. Bos, J. de Rooij, and K. A. Reedquist, Rap1 signalling: adhering to new models, Nat. Rev. Mol. Cell Biol. 2 (2001) 369-377.

[2] T. Kinashi, Intracellular signalling controlling integrin activation in lymphocytes, Nat. Rev. Immunol. 5 (2005) 546-559.

[3] M. Duchniewicz, T. Zemojtel, M. Kolanczyk, S. Grossmann, J. S. Schede, and F. J. Zwartkruis, Rap1A-deficient T and B cells show impaired integrin-mediated cell adhesion, Mol. Cell. Biol. 26 (2006) 643-653.

[4] M. Chrzanowska-Wodnicka, S. S. Smyth, S. M. Schoenwaelder, T. H. Fischer, and G. C. White, Rap1b is required for normal platelet function and hemostasis in mice, J. Clin. Invest. 115 (2005) 680-687.

[5] Y. Liao, K. Kariya, C.-D. Hu, M. Shibatohge, M. Goshima, T. Okada, Y. Watari, X. Gao, T.-G. Jin, Y. Yamawaki-Kataoka, and T. Kataoka, RA-GEF, a novel Rap1A guanine nucleotide exchange factor containing a Ras/Rap1A-associating domain, is conserved between nematode and humans, J. Biol. Chem. 274 (1999) 37815-37820.

[6] Y. Liao, T. Satoh, X. Gao, T.-G. Jin, C.-D. Hu, and T. Kataoka, RA-GEF-1, a guanine nucleotide exchange factor for Rap1, is activated by translocation induced by association with Rap1·GTP and enhances Rap1-dependent B-Raf activation, J. Biol. Chem. 276 (2001) 28478-28483.

[7] X. Gao, T. Satoh, Y. Liao, C. Song, C.-D. Hu, K. Kariya, and T. Kataoka, Identification and characterization of RA-GEF-2, a Rap guanine nucleotide exchange factor that serves as a downstream target of M-Ras, J. Biol. Chem. 276 (2001) 42219-42225.

[8] Y. Ohba, K. Ikuta, A. Ogura, J. Matsuda, N. Mochizuki, K. Nagashima, K. Kurokawa, B. J. Mayer, K. Maki, J. Miyazaki, and M. Matsuda, Requirement for C3G-dependent Rap1 activation for cell adhesion and embryogenesis, EMBO J. 20 (2001) 3333-3341.

[9] J. R. Crittenden, W. Bergmeier, Y. Zhang, C. L. Piffath, Y. Liang, D. D. Wagner, D. E. Housman, and A. M. Graybiel, CalDAG-GEFI integrates signaling for platelet aggregation and thrombus formation, Nat. Med. 10 (2004) 982-986.

[10] Y. Yoshikawa, T. Satoh, T, Tamura, P. Wei, S. E. Bilasy, H. Edamatsu, A. Aiba, K. Katagiri, T. Kinashi, K. Nakao, and T. Kataoka, The M-Ras-RA-GEF-2-Rap1 pathway

mediates tumor necrosis factor alpha dependent regulation of integrin activation in splenocytes, Mol. Biol. Cell 18 (2007) 2949-2959.

[11] K. Sakai, and J. Miyazaki, A transgenic mouse line that retains Cre recombinase activity in mature oocytes irrespective of the cre transgene transmission, Biochem. Biophys. Res. Commun. 237 (1997) 318-324.

[12] M. Tadano, H. Edamatsu, S. Minamisawa, U. Yokoyama, Y. Ishikawa, N. Suzuki, D. Wu, M. Masago-Toda,, Y. Yamawaki-Kataoka, T. Setsu, T. Terashima, S. Maeda, T. Satoh, and T. Kataoka, Congenital semilunar valvulogenesis defect in mice deficient in phospholipase C epsilon, Mol. Cell. Biol. 25 (2005) 2191-2199.

[13] D. Wu, M. Tadano, H. Edamatsu, M. Masago-Toda, Y. Yamawaki-Kataoka, T. Terashima, A. Mizoguchi, Y. Minami, T. Satoh, and T. Kataoka, Neuronal lineage-specific induction of phospholipase C epsilon expression in the developing mouse brain, Eur. J. Neurosci. 17 (2003) 1571-1580.

[14] T. M. Schlaeger, Y. Qin, Y. Fujiwara, J. Magram, and T. N. Sato, Vascular endothelial cell lineage-specific promoter in transgenic mice, Development 121 (1995) 1089-1098.

[15] J. T. Yang, H. Rayburn, and R. O. Hynes, Cell adhesion events mediated by alpha 4 integrin are essential in placental and cardiac development, Development 121 (1995) 549-560.

[16] L. Kwee, H. S. Baldwin, H. M. Shen, C. L. Stewart, C. Buck, C. A. Buck, and M. A. Labow, Defective development of the embryonic and extraembryonic circulatory systems in vascular cell adhesion molecule (VCAM-1) deficient mice, Development 121 (1995) 489-503.

[17] W. Risau, Differentiation of endothelium, FASEB J. 9 (1995) 926-933.

[18] M. C. Dickson, J. S. Martin, F. M. Cousins, A. B. Kulkarni, S. Karlsson, and R. J. Akhurst, Defective haematopoiesis and vasculogenesis in transforming growth factor-beta 1 knock out mice, Development 121 (1995) 1845-1854.

[19] J. Rossant, and J. C. Cross, Placental development: lessons from mouse mutants, Nat. Rev. Genet. 2 (2001) 538-548.

[20] W. Risau, Mechanisms of angiogenesis, Nature 386 (1997) 671-674.

[21] A. Sakurai, S. Fukuhara, A. Yamagishi, K. Sako, Y. Kamioka, M. Masuda, Y. Nakaoka, and N. Mochizuki, MAGI-1 is required for Rap1 activation upon cell-cell contact and for enhancement of vascular endothelial cadherin-mediated cell adhesion, Mol. Biol. Cell 17 (2006) 966-976.

[22] S. Fukuhra, A. Sakurai, A. Yamagishi, K. Sako, N. Mochizuki, Vascular endothelial cadherin-mediated cell-cell adhesion regulated by a small GTPase, Rap1, J. Biochem. Mol. Biol. 39 (2006) 132-139.

[23] W. Pellis-van Berkel, M. H. Verheijen, E. Cuppen, M. Asahina, J. de Rooij, G. Jansen, R. H. Plasterk, J. L. Bos , and F. J. Zwartkruis, Requirement of the Caenorhabditis elegans RapGEF pxf-1 and rap-1 for epithelial integrity, Mol. Biol. Cell 16 (2005) 106-116.

[24] S. Huelsmann, C. Hepper, D. Marchese, C. Knoll, and R. Reuter, The PDZ-GEF dizzy regulates cell shape of migrating macrophages via Rap1 and integrins in the Drosophila embryo, Development 133 (2006) 2915-2924

[25] E. L. George, H. S. Baldwin, and R. O. Hynes, Fibronectins are essential for heart and blood vessel morphogenesis but are dispensable for initial specification of precursor cells, Blood 90 (1997) 3073-3081.

[26] J. T. Yang, H. Rayburn, and R. O. Hynes, Embryonic mesodermal defects in alpha 5 integrin-deficient mice, Development 119 (1993) 1093-1105.

[27] S. Gory-Fauré, M. H.Prandini, H. Pointu, V. Roullot, I. Pignot-Paintrand, M. Vernet, and P. Huber, Role of vascular endothelial-cadherin in vascular morphogenesis, Development 126 (1999) 2093-2102.

[28] G. L. Radice, H. Rayburn, H. Matsunami, K. A.Knudsen, M. Takeichi, and R. O. Hynes, Dev Biol. 181 (1997) 64-78.

Figure Legends

Fig. 1. Targeted disruption of the mouse *RA-GEF-1* gene. (A) schematic representation of the wild-type allele (*RA-GEF-1*$^{+}$), the targeting vector, the floxed allele (*RA-GEF-1*^{flox}) and the disrupted allele (*RA-GEF-1*$^{-}$). Exons (*black rectangles,* intact exons; *white rectangle,* the

targeted exon 15), loxP sites (*black triangles*), *TK-neo* (*Neo*) and the diphtheria toxin A chain (*DT-A*) cassettes are indicated. Positions of the 5', 3' and *neo* probes for Southern blot analysis are shown below the gene structures. Locations of the primers p1, p2 and p3 for PCR genotyping and various restriction endonuclease cleavage sites (A, *Apa*I; Ba, *Bam*HI; Bs, *Bsp*120I; H, *Hind*III; Nh, *Nhe*I; No, *Not*I; P, *Pml*I) are shown above the gene structures. (B) genotyping of ES cell clones. Genomic DNAs (5 μg each) were cleaved with *Bam*HI (for 5' and *Neo* probes) or *Nhe*I (for 3' probe) and subjected to Southern blot hybridization. The positions and estimated sizes of the hybridization signals are shown. (C) genotyping of the mutant mice. Genomic DNAs (5 μg each) were cleaved with *Bam*HI and subjected to Southern blot hybridization with the 5' probe (*left panel*). Genomic DNAs were also analyzed by PCR employing a primer pair of p1 and p2 (*right upper panel*) or a pair of p1 and p3 (*right lower panel*). (D) genotypes of E10.5 embryos were determined by PCR as described in (C) using yolk sac genomic DNAs.

Fig. 2. Morphological comparison of wild-type and *RA-GEF-1*$^{-/-}$ embryos from cross-breeding of *RA-GEF-1*$^{-/-}$ mice. (A) lateral views of two *RA-GEF-1*$^{-/-}$ embryos (-/-) and a littermate wild-type embryo (+/+) at E8.5. The positions of head folds (*hf*) are shown by *arrows*. Scale bar = 500 μm. (B) dorsal views of *RA-GEF-1*$^{-/-}$ embryos (-/-) and a littermate wild-type embryo (+/+) at E9.5 dissected free from yolk sacs. Neural tubes (*nt*) are shown by *arrows*. Scale bar = 500 μm. (C) whole-mount views of an *RA-GEF-1*$^{-/-}$ embryo (-/-) and a littermate wild-type embryo (+/+) at E9.5, and magnified views of their yolk sacs (*lower panels*). Large vitelline blood vessels are indicated by *arrowheads*. Embryos proper (*em*), yolk sacs (*ys*) and deciduas (*de*) are shown. Scale bar = 500 μm. (D) detection of the RA-GEF-1 protein in E10.5 embryos. Protein extracts (approximately 20 μg protein each) from whole E10.5 embryos were subjected to Western blot analysis with anti-mouse RA-GEF-1 and anti-mouse α-actin antibodies. The position and estimated molecular size of RA-GEF-1 are shown. (E) the time course of RA-GEF-1 expression. Total RNAs from wild-type whole embryos were subjected to RT-PCR for the detection of *RA-GEF-1* and *glyceraldehyde 3-phosphate dehydrogenase (GAPDH)* mRNAs (*upper two panels*). The

number of PCR amplification cycles was 25. Protein extracts from wild-type whole embryos were subjected to Western blot analysis with anti-mouse RA-GEF-1 and anti-mouse α-actin antibodies (*lower two panels*). (F) immunofluorescence staining with anti-RA-GEF-1 (*green*) and anti-PECAM-1 (*red*) antibodies on sagittal sections of wild-type yolk sacs at E8.5. Endodermal layers (*end*), mesodermal layers (*mes*) and blood cells (*bc*) are indicated. Strong expression of RA-GEF-1 is indicated by *arrows*. *Arrowheads* indicate PECAM-1-positive areas. Scale bar = 20 μm.

Fig. 3. Vascular defects in *RA-GEF-1*$^{-/-}$ embryos, yolk sacs and placentas. (A) whole-mount immunostaining with anti-PECAM-1 antibody of two *RA-GEF-1*$^{-/-}$ embryos (-/-) and a wild-type embryo (+/+) at E9.5. Cranial vessels (*cv*), otic vesicle (*ov*), heart (*he*), dorsal aorta (*da*), and intersomitic vessels (*is*) are indicated by *black arrows*. The first, second and third aortic arches are shown by numbers *1, 2,* and *3,* respectively. A strongly stained bulbous allantois is indicated by *black arrowhead.* The hypomorphic intersomitic vessels and local primary vascular plexuses in *RA-GEF-1*$^{-/-}$ embryos are indicated by *red arrows* and *arrowheads,* respectively. Scale bar = 500 μm. (B) PECAM-1 staining of an *RA-GEF-1*$^{-/-}$ yolk sac (-/-) and a littermate wild-type yolk sac (+/+) at F9.5. *Arrowheads* indicate PECAM-1-positive signals. Scale bars = 500 μm. (C) HE staining of the transverse sections of an *RA-GEF-1*$^{-/-}$ yolk sac (-/-) and a littermate wild-type yolk sac (+/+) at E8.5 (*a-d*) and E9.5 (*e-h*). Magnified views of the *boxed* areas of *a, b, e,* and *f* are shown in *c, d, g,* and *h,* respectively. Endodermal layers (*end*), mesodermal layers (*mes*) and blood cells (*bc*) are shown by *arrowheads*. Endothelial layers (*et*) are shown by *arrows*. Scale bar = 100 μm. (D) HE staining of the sagittal sections of an *RA-GEF-1*$^{-/-}$ placenta (-/-) and a littermate wild-type placenta (+/+) at E9.5. Magnified views of the *boxed* area of *left panels* are shown in *right panels*. *Arrows* indicate fetal blood vessels, and *arrowheads* indicate maternal blood sinuses. Deciduas (*da*), giant trophoblast layer (*gt*), labyrinthine layer (*la*), and chorionic plate (*cp*) are shown. Scale bars in *left* and *right panels* are 500 μm and 100 μm, respectively.

Table 1. *Genotype of progeny cross-breeding of RA-GEF-1*$^{+/-}$ *mice*

Developmental stage	No. of animals (%) of genotype [a]			Total
	+/+	+/-	-/-	
E8.5	19(30)	30(47)	15(23)	64(100)
E9.5	16(25)	37(57)	12(18)	65(100)
E10.5-12.5	13(22)	39(65)	8(13)	60(100)
E13.5-15.5	8(35)	15(65)	0	23(100)
P21	62(36)	112(64)	0	174(100)

[a] Number are given with percentage in parenthesis

E, embryonic day

P, postnatal day

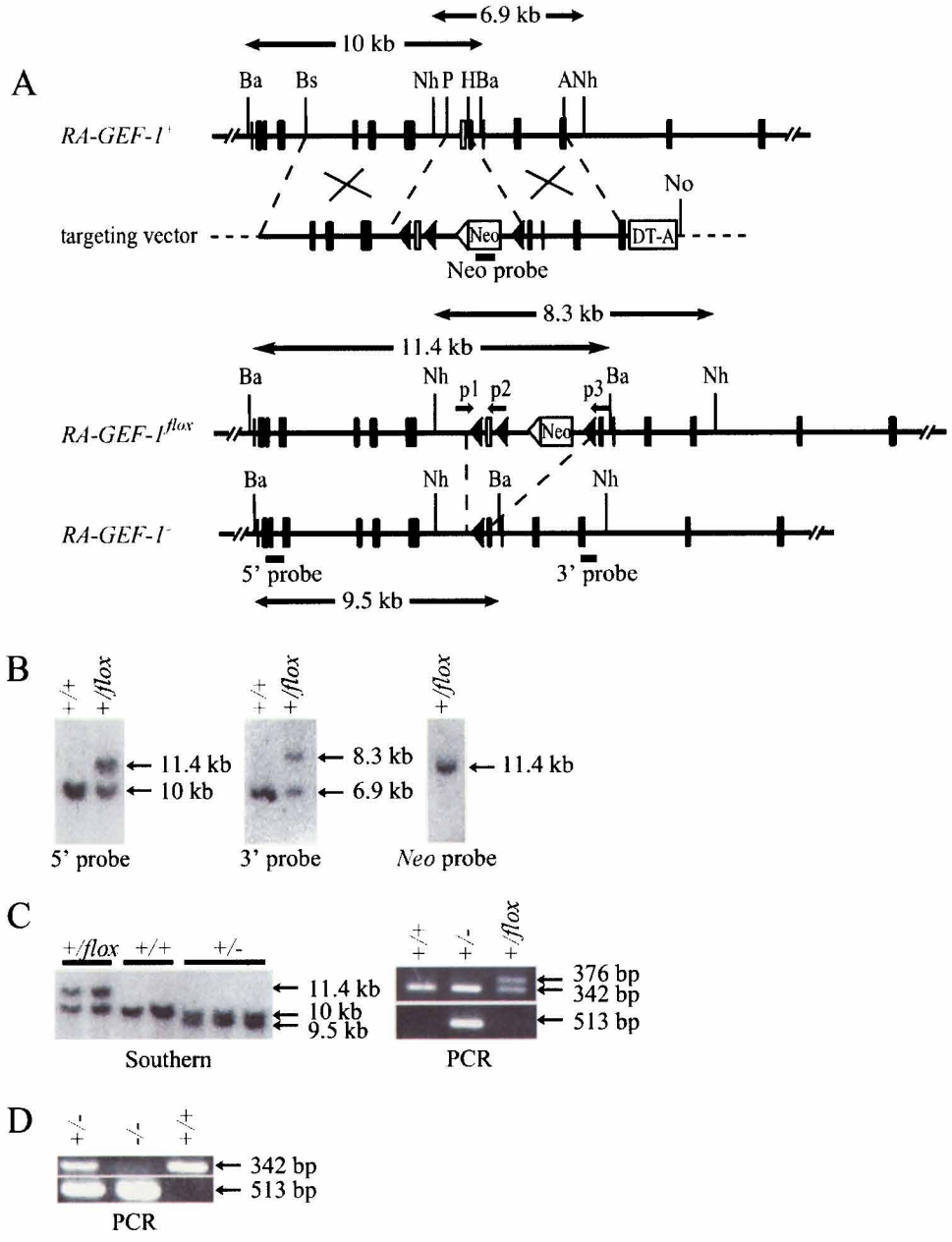
A
6.9 kb
10 kb
Ba
Bs
Nh P HBa
ANh
RA-GEF-1+
No
targeting vector
Neo
DT-A
Neo probe
8.3 kb
11.4 kb
Ba
Nh
p1 p2
p3
Ba
Nh
RA-GEF-1flox
Neo
Ba
Nh
Ba
Nh
RA-GEF-1-
5' probe
3' probe
9.5 kb
B
+/+
+/flox
11.4 kb
10 kb
8.3 kb
6.9 kb
11.4 kb
5' probe
3' probe
Neo probe
C
+/flox
+/+
+/-
11.4 kb
10 kb
9.5 kb
Southern
+/+
+/-
+/flox
376 bp
342 bp
513 bp
PCR
D
+/-
-/-
+/+
342 bp
513 bp
PCR

Fig. 1

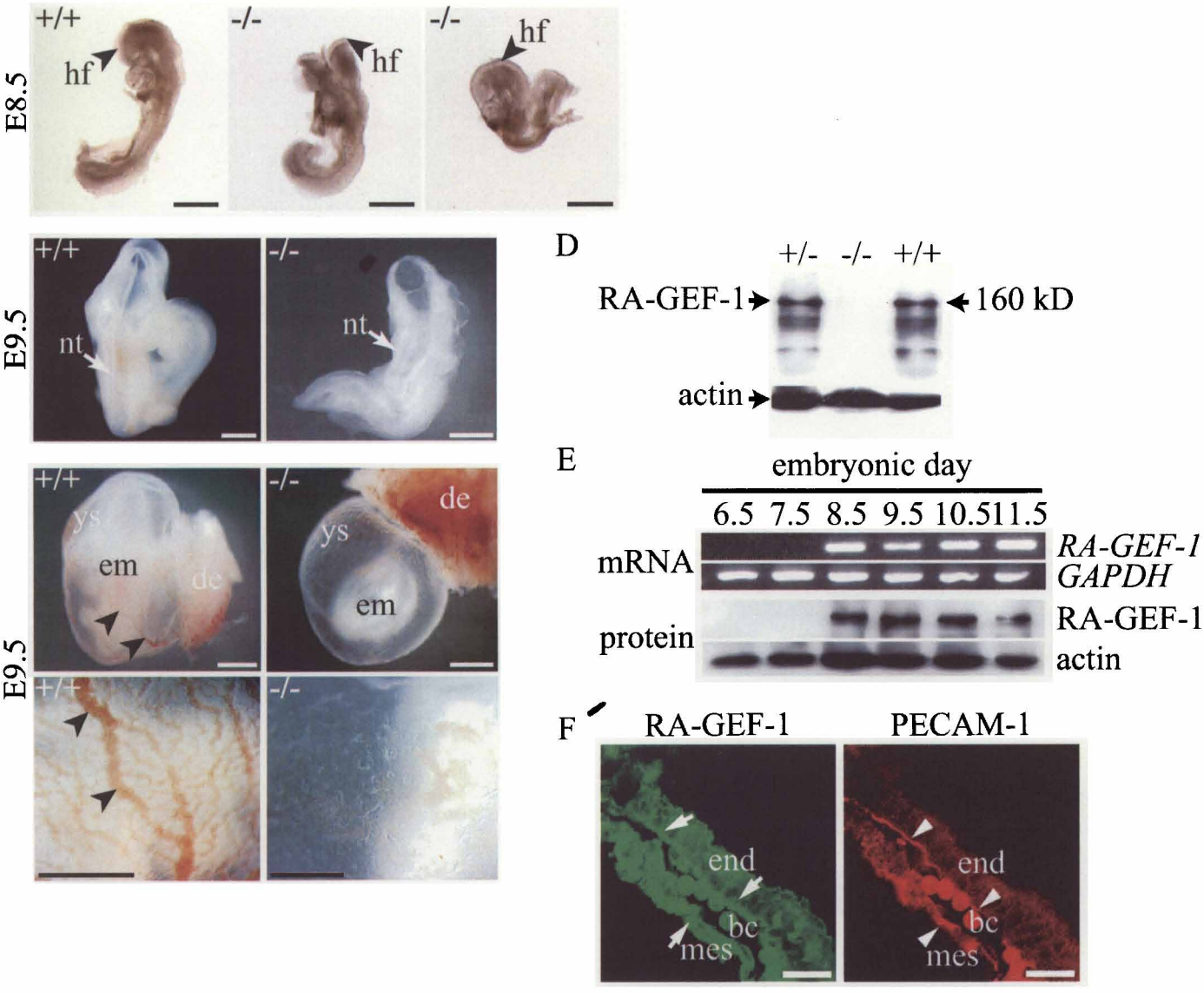
E8.5
+/+
hf
-/-
hf
-/-
hf
E9.5
+/+
nt
-/-
nt
E9.5
+/+
ys
em
de
-/-
de
ys
em
+/+
-/-
D
+/-
-/-
+/+
RA-GEF-1
160 kD
actin
E
embryonic day
6.5 7.5 8.5 9.5 10.5 11.5
mRNA
RA-GEF-1
GAPDH
protein
RA-GEF-1
actin
F
RA-GEF-1
PECAM-1
end
bc
mes
end
bc
mes

Fig. 2

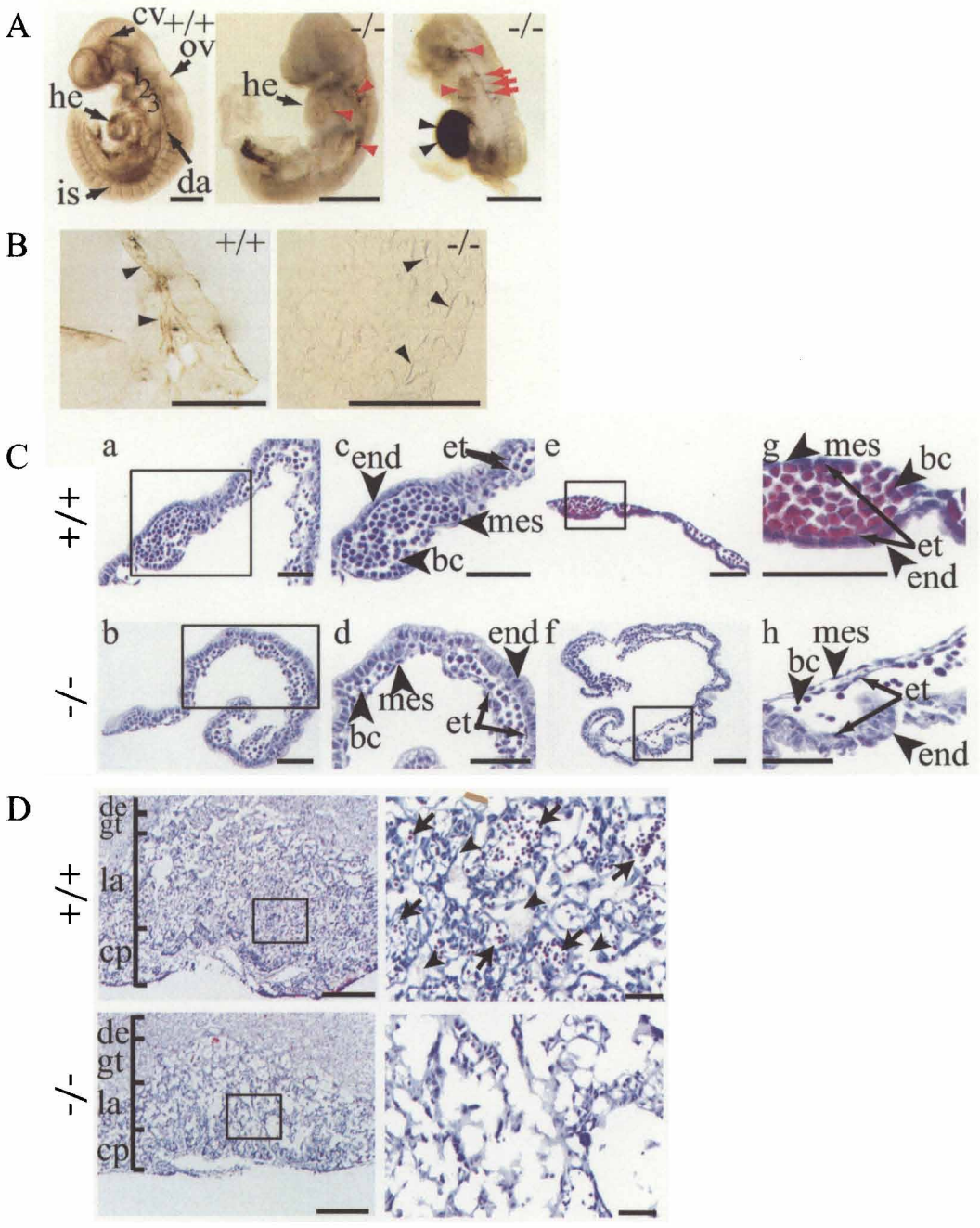
A
cv
+/+
ov
he
1
2
3
is
da
he
-/-
-/-
B
+/+
-/-
C
+/+
a
c
end
et
e
mes
bc
g
mes
bc
et
end
-/-
b
d
end
f
mes
bc
et
h
mes
bc
et
end
D
+/+
de
gt
la
cp
-/-
de
gt
la
cp

Fig. 3